Microsc. Microanal. 9, 144–151, 2003
DOI: 10.1017/S1431927603030204

Microscopy AND Microanalysis

© MICROSCOPY SOCIETY OF AMERICA 2003

# Cathodoluminescence Efficiency Dependence on Excitation Density in n-Type Gallium Nitride

Matthew R. Phillips,[1]* Hagen Telg,[1] Sergei O. Kucheyev,[2] Olaf Gelhausen,[1] and Milos Toth[3]

[1]*Microstructural Analysis Unit, University of Technology, Sydney, Broadway, NSW, 2007, Australia*
[2]*Department of Electronic Materials Engineering, RSPhysSE, The Australian National University, Canberra, ACT, 0200, Australia*
[3]*Cavendish Laboratory, University of Cambridge, Madingley Road, Cambridge, CB3 0HE, United Kingdom*

**Abstract:** Cathodoluminescence (CL) spectra from silicon doped and undoped wurtzite n-type GaN have been measured in a SEM under a wide range of electron beam excitation conditions, which include accelerating voltage, beam current, magnification, beam diameter, and specimen temperature. The CL intensity dependence on excitation density was analyzed using a power-law model ($I_{CL} \propto J^m$) for each of the observed CL bands in this material. The yellow luminescence band present in both silicon and undoped GaN exhibits a close to cube root ($m = 0.33$) dependence on electron beam excitation at both 77 K and 300 K. However, the blue (at 300 K) and donor-acceptor pair (at 77 K) emission peaks observed in undoped GaN follow power laws with exponents of $m = 1$ and $m = 0.5$, respectively. As expected from its excitonic character, the near band edge emission intensity depends linearly ($m = 1$) in silicon doped GaN and superlinearly ($m = 1.2$) in undoped GaN on the electron beam current. Results show that the intensities of the CL bands are highly dependent not only on the defect concentration but also on the electron-hole pair density and injection rate. Furthermore, the size of the focussed electron beam was found to have a considerable effect on the relative intensities of the CL emission peaks. Hence SEM parameters such as the objective lens aperture size, astigmatism, and the condenser lens setting must also be considered when assessing CL data based on intensity measurements from this material.

**Key words:** cathodoluminescence, gallium nitride, excitation density

## Introduction

Cathodoluminescence (CL) analysis in a scanning electron microscope (SEM) is a very powerful technique used extensively to study the optical and electronic properties of defects in semiconductor materials and devices at high spatial resolution (Yacobi and Holt, 1990). Recently, the CL technique has been applied to the investigation of gallium nitride (GaN) thin films, which are utilized in a broad range of technological applications, including UV-blue light emitting diodes and lasers, UV detectors, and high-power/temperature and high-speed electronic devices. In GaN, a typical CL spectrum exhibits a near edge emission (NBE) with a maximum around 3.38 eV at 300 K, broad yellow (YL) and blue (BL) defect related bands centred on ~2.15 eV and ~2.9 eV, respectively at 300 K and a donor acceptor pair (DAP) emission centered on ~3.28 eV at 77 K (Orton and Foxon, 1998). Although considerable debate surrounds the exact origin of these defect-induced emissions, there is

Received February 12, 2002; accepted April 16, 2002.
Hagen Telg is on leave from Festörperinstitut, Technische Universität, Berlin, Germany.
**Corresponding author*. E-mail: matthew.phillips@uts.edu.au

reasonable theoretical and experimental evidence to support the involvement of the native gallium vacancy- ($V_{Ga}^{3-}$) related defects and their complexes with shallow donors and hydrogen (Neugebauer and Van de Walle, 1996).

The depth distribution of defects throughout a GaN epilayer can be determined nondestructively by measuring CL spectra as a function of the electron penetration range. This type of CL analysis is generally conducted by systematically varying the electron beam energy ($E_O$), while adjusting the beam current ($I_B$) to maintain a constant beam power ($E_O I_B$). In this way, CL spectra can be collected with the same electron-hole pair injection rate from different depths within the specimen. These data can then be analyzed by comparing the depth-resolved CL measurements with modeled electron energy loss profiles simulated using Monte Carlo techniques (Fleischer et al., 1999; Gelhausen et al., 2001). However, correct interpretation of experimental depth-resolved data is only possible when the intensity dependence of each CL band on the electron-hole pair injection rate is known. It is the purpose of this work to investigate (i) the excitation current dependency of the CL emission in GaN, and (ii) the influence of the SEM magnification, scan rate, and the electron beam spot size on CL emission. The results demonstrate the importance of considering CL excitation dependences in GaN when assessing defect concentration and distribution or when comparing n-type GaN specimens on the basis of CL spectra.

## Materials and Methods

In this study, 5 × 5-mm squares were carefully snapped from 50-mm-diameter wafers of ~2-$\mu$m-thick Si-doped ($n_e = \sim 10^{18}$ cm$^{-3}$) and nominally undoped GaN ($n_e = \sim 10^{16}$ cm$^{-3}$) grown in EMCORE reactors on (0001) sapphire substrates by metal organic chemical vapor deposition. Cathodoluminescence measurements were conducted at 77 K and 300 K using an Oxford Instruments MonoCL2 installed on a JEOL 35C scanning electron microscope (SEM) equipped with a liquid nitrogen cold stage. Light was collected with a semiparabolic mirror containing an electron beam access hole located directly above its focus point. All CL spectra were collected with the specimen positioned at the focal plane of the mirror. The CL signal was dispersed by a 1200 lines/mm grating blazed at 500 nm and measured with a Hamamatsu R943-02 Peltier cooled photomultiplier tube.

CL spectra were collected using a reduced-area raster scan (line dwell time 0.54 ms and line scan time 0.26 ms) with a scan rate of 10 frames per second. The frame area ranged between (90 × 102) $\mu$m$^2$ and (3 × 3.4) $\mu$m$^2$ by SEM magnification adjustments. The scan area was accurately measured at each magnification using a calibration mesh. The electron-hole pair injection dose-rate was varied by (i) changing the $I_B$ in a focused probe at a fixed $E_O$, and (ii) changing the electron beam spot size ($d_P$) at a fixed $I_B$ and $E_O$ by defocusing the objective lens. A fresh area of specimen was used for each CL measurement. The electron beam current was measured using a Faraday cup suitably designed to accommodate an electron beam probe with a $d_P \leq 200$ $\mu$m. To investigate the CL excitation dependence on the diameter of the focused electron beam, CL spectra were measured at the same $E_O I_B$ using two different objective lens aperture diameters (300 $\mu$m and 600 $\mu$m). The diameter of the electron probe was determined by measuring the width of a carbon contamination spot deposited during 100-s spot mode irradiation. The time dependence of the CL emission on injection dose rate was investigated using time-resolved CL spectroscopy measurements. CL spectra were corrected for the wavelength response of the complete CL collection system and converted to an energy scale by multiplying $I_{CL}(\lambda)$ by $\lambda^2$.

## Results and Discussion

Typical CL spectra (20 keV at 77 K), exhibiting the YL, BL, DAP, and NBE bands for undoped and silicon-doped GaN specimens are shown in Figure 1. The intensity of each of these bands was observed to increase at a different rate as the beam current was increased from 0.01 nA to 100 nA. This behavior is illustrated in Figure 2a for the Si-doped GaN specimen, which shows the intensity of the NBE and YL versus $I_B$ at 300 K and Figure 2b at 77 K. The $I_{CL}$ excitation density dependence on $I_B$ has been analyzed for each specimen at 77 K and 300 K using a simple power-law model where the CL intensity ($I_{CL}$) and excitation power $J_B$ are related by ($I_{CL} \propto J^m$). Power-law fits, shown in Figure 2 by straight lines, reveal that the intensities of the YL and DAP emission bands display a strongly sublinear dependence on $I_B$, with $I_{CL}^{YL} \propto I_B^{0.28}$ and $I_{CL}^{DAP} \propto I_B^{0.46}$ at 77 K. The intensity of the BL defect-related band in the undoped GaN, however, exhibits a linear power-law relationship ($I_{CL}^{BL} \propto I_B^{1.08}$) with the excitation level at 300 K. The NBE

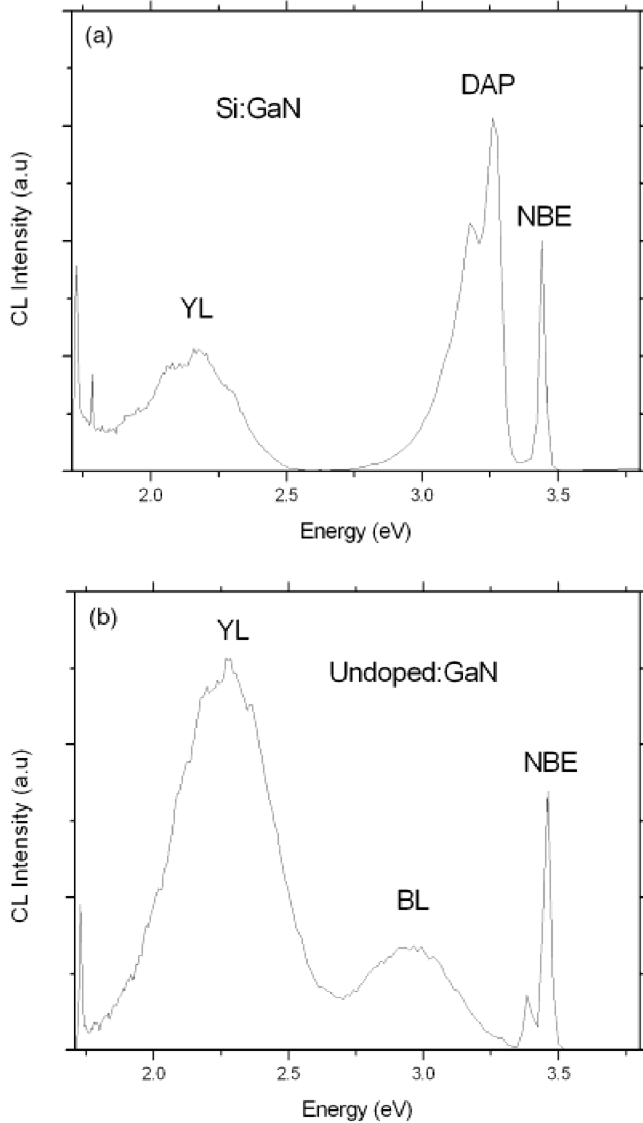


**Figure 1.** Typical CL spectra from (**a**) silicon-doped and (**b**) undoped GaN at 77 K exhibiting the YL, BL, DAP, and NBE emission bands ($E_O$ = 20 kV, $I_B$ = 1 nA, CL bandpass = 2.5 nm, and scan size = 90 × 102 $\mu$m$^2$).

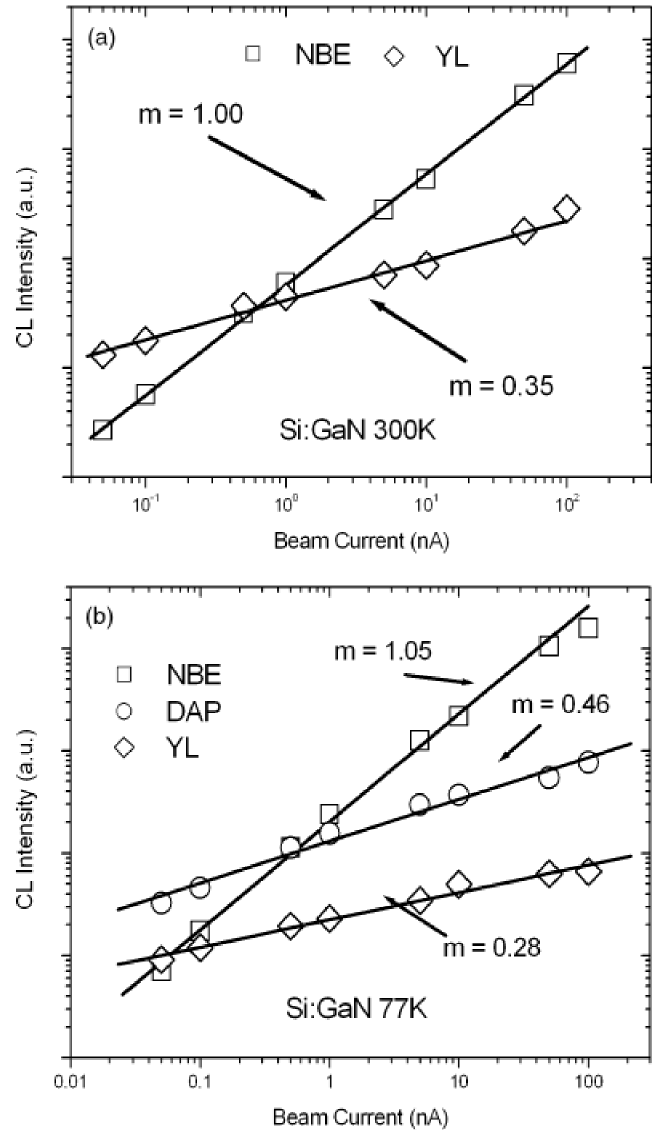


**Figure 2.** Intensities of the NBE and YL measured from a silicon-doped GaN specimen at (**a**) 300 K and (**b**) 77 K as a function of $I_B$ with a finely focused electron beam ($E_O$ = 20 kV, CL bandpass = 2.5 nm, and scan size = 90 × 102 $\mu$m$^2$).

bands show linear ($I_{CL}^{NBE} \propto I_B^{1.0}$) and superlinear ($I_{CL}^{NBE} \propto I_B^{1.2}$) dependencies on $I_B$ for GaN:Si and undoped GaN, respectively. It is worth noting that a superlinear ($I_{CL}^{NBE} \propto I_B^{1.16}$) dependence on $I_B$ was observed in Si-doped GaN when the measurements were collected from the same region of the specimen, indicating beam-induced CL enhancement. All power-law exponents measured in this work are summarized in Table 1, and these values were found to vary within experimental error for measurements at both 20 keV (see Table 1) and 10 keV.

The measured power-law exponents for the NBE emission in both the silicon and undoped GaN specimens are consistent with CL emission associated with excitonic recombination processes (Pankove, 1975). In undoped GaN, the superlinear dependence of the NBE on excitation level is characteristic of recombination channels related to free and bound excitons, while the linear NBE power-law relationship exhibited in the Si-doped GaN is typically observed with an intrinsic (i.e., band-to-band transition) recombination process (Mullhauser et al., 1996). The sublinear depen-

**Table 1.** Power Law Exponents, $m$, for the $I_{CL} \propto I_B^m$ Excitation Density Dependence on $I_B$ and the Observed Time-Dependent Behavior of the CL Peaks in n-Type GaN

| Si-doped GaN (20 kV) | | | |
|---|---|---|---|
| | NBE | YL | DAP |
| RT (same region) | 1.16 ± 0.01 | 0.34 ± 0.01 | |
| RT (fresh region) | 1.01 ± 0.01 | 0.35 ± 0.02 | |
| LN (fresh region) | 1.05 ± 0.03 | 0.27 ± 0.01 | 0.46 ± 0.02 |
| Kinetics RT (1 nA) | none | none | |
| Kinetics RT (100 nA) | none | slight increase | |
| Kinetics LN (1 nA) | none | none | none |
| Kinetics LN (100 nA) | none | slight increase | linear increase |
| **Undoped GaN (20 kV)** | | | |
| | NBE | YL | BL |
| RT (fresh region) | 1.20 ± 0.03 | 0.35 ± 0.01 | 1.08 ± 0.03 |
| LN (fresh region) | 1.08 ± 0.02 | unstable | unstable |
| RT Kinetics (1 nA) | none | none | none |
| RT Kinetics (100 nA) | none | large slow increase | large slow increase |
| LN Kinetics (1 nA) | none | slow increase | slow decrease |
| LN Kinetics (100 nA) | none | rapid increase then decrease | very rapid decrease |

dencies of the YL and DAP on $I_B$ can be qualitatively explained by saturation of a finite number of radiative recombination centers. Simple rate equation models that allow for saturation of luminescence centers predict power-law exponents of 0.5, 1.0, and 1.5, depending on the defect concentration and excitation power. The measured square root dependence of the DAP band on $I_B$ is in agreement with these models and photoluminescence excitation density measurements which report a square root dependence (Singh et al., 1994; Grieshaber et al., 1996; Reshchikov and Korokov, 2001). However, the CL intensity of the YL band exhibits a cube root dependence on $I_B$. This discrepancy between the measured CL and PL power-law exponents can be attributed to either (i) the orders-of-magnitude greater electron-hole pair density and generation rate for electron excitation, compared with typical values for optical excitation, or (ii) variation in the YL emission intensity with increasing $I_B$ due to electron beam induced effects.

Time-resolved CL spectroscopy measurements conducted under low (1 nA) and high (100 nA) excitation at 77 K and 300 K for both silicon and undoped GaN are shown in Figure 3. Time-dependent irradiation-induced effects on the CL and PL intensity have been attributed to diffusion of $O_N^+$ and $H^+$ (Toth et al., 1999), carbon contamination (Toth et al., 1999), repulsive space charge at structural dislocations (Kim et al., 1999), and surface annealing (Herrera Zaldivar et al., 1998). However, in the context of the present work, knowledge of the exact nature of the mechanisms involved in these processes is not necessary, and it is sufficient to know merely the excitation conditions under which the CL intensity is stable during electron irradiation. The CL intensity of the NBE peak and YL band in both Si doped and undoped GaN is constant with time under all current injection levels at 300 K (Fig. 3a) except for high $I_B$ in undoped GaN, where both the YL and BL bands increase slowly with irradiation time (Fig. 3c). At 77 K, the intensity of the YL band and NBE peak in the Si-doped GaN sample are stable with time at all $I_B$ values, and the DAP intensity rises very slowly only under high current injection (Fig. 3b). The temporal behavior of YL and BL bands in the undoped GaN samples, however, is strongly dependent on $I_B$, particularly at 77 K, as shown in Figure 3d. At this temperature, under high injection currents, an extremely rapid decrease in the BL intensity is observed with time, whereas the YL quickly increases, then decreases, over the same time interval. A complete summary of the CL kinetics results is presented in Table 1. These CL kinetics studies clearly demonstrate that the electron-beam

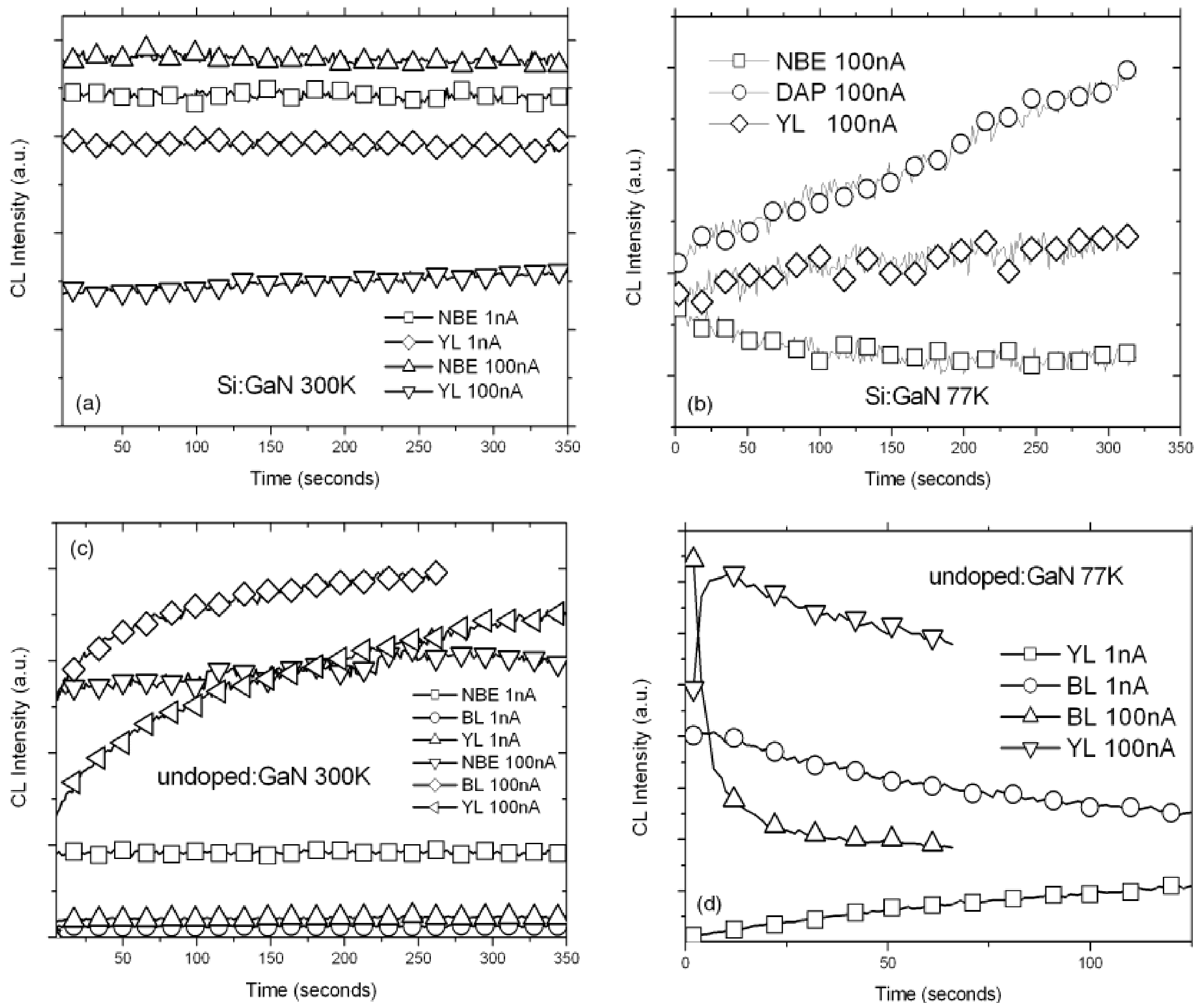


**Figure 3.** Time dependence of the NBE, YL, DAP, and BL bands in (**a**) silicon-doped GaN at 300 K, (**b**) silicon-doped GaN at 77 K, (**c**) undoped at GaN 300 K, and (**d**) undoped GaN at 77 K ($E_O = 20$ kV, CL bandpass = 2.5 nm, and scan size = $90 \times 102\ \mu m^2$).

induced, time-dependent behavior of the CL emission in silicon and undoped GaN cannot account for the cube root dependence on $I_B$ for the YL band at 300 K.

The dependence of the intensity of the YL and NBE on electron beam spot size, $d_B$, (i.e., power density) in silicon-doped GaN is shown in Figure 4. This behavior of the YL band can be attributed to its highly nonlinear dependence on excitation density. The results may also suggest that, as the YL emission centers saturate with increasing $I_B$, excess carriers are then free to recombine via excitonic pathways, leading to an increase in the NBE emission and an anticorrelation with the YL dependence on $d_B$, as observed. However, this interpretation cannot be correct, since the NBE band exhibits a linear power-law relationship with the excitation level. A more plausible explanation for the NBE intensity dependence on $d_B$ involves competitive recombination with nonradiative surface states, which exhibit a nonlinear dependence on power density. This is not surprising, as the NBE emission is only detected very close (nanometer scale) to the surface as a result of very efficient self-absorption in GaN, whereas the YL signal originates from much greater depths (micron scale) within the specimen (Fleischer et al., 1999).

The very strong dependence of the YL and NBE bands on $d_B$ means that the SEM parameters that determine $d_B$, such as the excitation level of the condenser lens, the

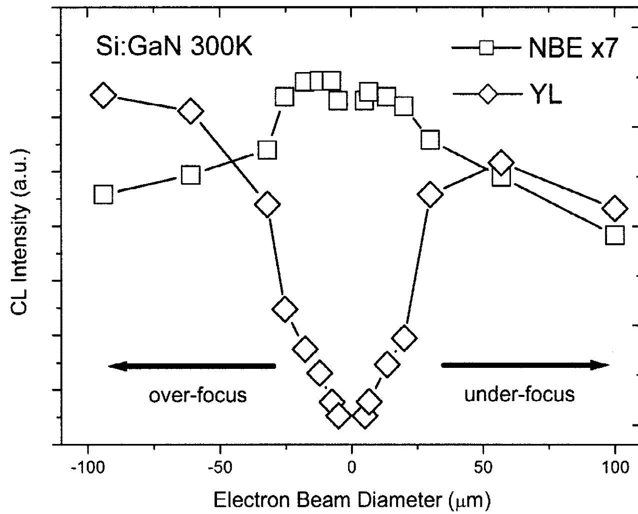


**Figure 4.** The dependence of the NBE and YL CL intensity in Si:GaN on electron beam diameter, $d_B$, which was varied by under- and overfocusing the objective lens in frame scan mode. The behavior of the YL band is attributed to its highly nonlinear dependence on excitation level, whereas the NBE response is tentatively ascribed to competitive recombination with nonradiative surface states, which exhibit a nonlinear dependence on the excitation level ($E_O = 20$ kV, $I_B = 1$ nA, CL bandpass = 2.5 nm, and scan size = $90 \times 102\ \mu m^2$).

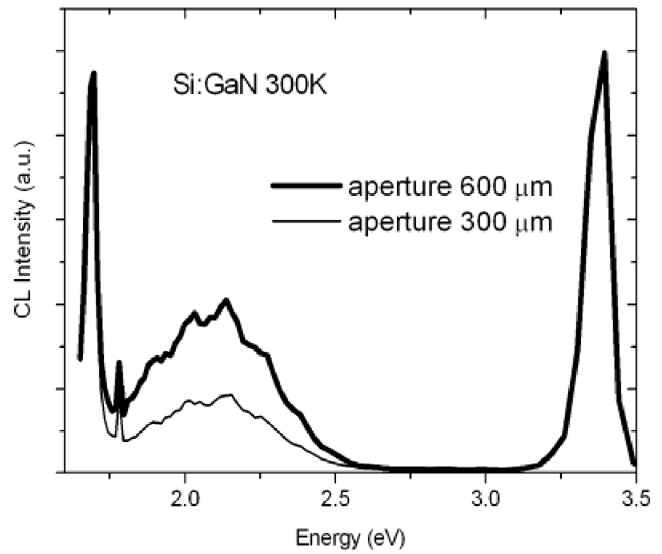


**Figure 5.** Dependence of YL CL intensity in Si:GaN on $d_B$. CL spectra were measured at the same beam power ($E_O I_B$) with a larger $d_B$ as the objective lens aperture is increased from 300 $\mu$m to 600 $\mu$m ($E_O = 20$ kV, $I_B = 1$ nA, CL bandpass = 2.5 nm, and scan size = $90 \times 102\ \mu m^2$).

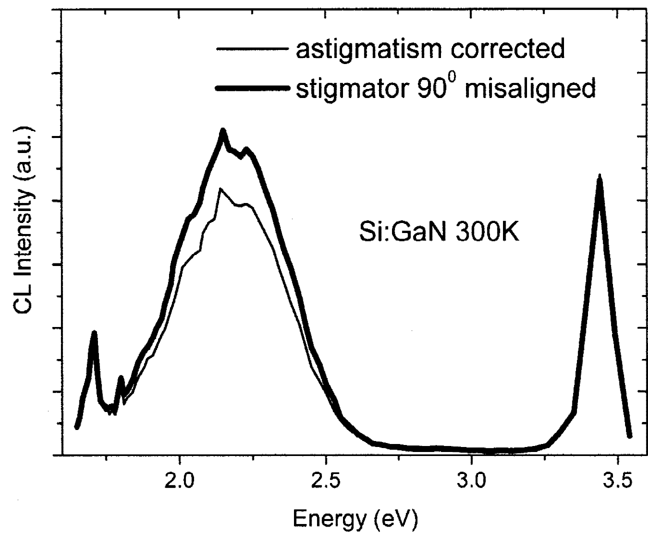


**Figure 6.** Dependence of YL CL intensity in Si:GaN on $d_B$. CL spectra were measured with the same beam power ($E_O I_B$) with a large $d_B$ as the $r, \theta$ stigmator was deliberately misaligned by $\theta = 90°$ from the astigmatism-corrected $\theta$ setting ($E_O = 20$ kV, $I_B = 1$ nA, CL bandpass = 2.5 nm, and scan size = $90 \times 102\ \mu m^2$).

diameter of the objective lens aperture, and proper correction for astigmatism (Goldstein et al., 1992) will significantly affect YL and NBE intensity. For example, it is seen in Figure 5 that the YL intensity increases when the objective lens aperture size is increased from 300 $\mu$m to 600 $\mu$m, even though the excitation power (20 keV, 1 nA) is constant. This behavior can be ascribed to broadening of $d_B$ due to an increased spatial contribution from spherical and chromatic aberrations, which both increase with aperture size. Similarly, $d_B$ is at a minimum when it is optimally corrected for astigmatism using the SEM stigmator controls. However, if the stigmator control is deliberately misaligned, a larger $d_B$ results, leading to an increase in the YL intensity, as shown in Figure 6. Furthermore, it is significant to note that the beam current is not constant as the objective lens is under- and overfocused due to the change in the electron beam crossover position with respect to the objective lens aperture. This effect is demonstrated in Figure 7, which shows $I_B$ as a function of objective lens current for objective lens aperture diameters of 120 $\mu$m, 300 $\mu$m, and 600 $\mu$m.

The dependence of the YL and NBE intensity on SEM magnification is shown in Figure 8. The behavior of YL and NBE bands is, in general terms, a direct consequence of their dependence on $d_B$ as described above. It is seen in Figure 9 that, as the SEM magnification ($M$) increases, the area scanned ($A$) on the specimen decreases as $A\ (\mu m^2) = 1.45 \times 10^9\ M^{-2}$. However, it is important to point out that,

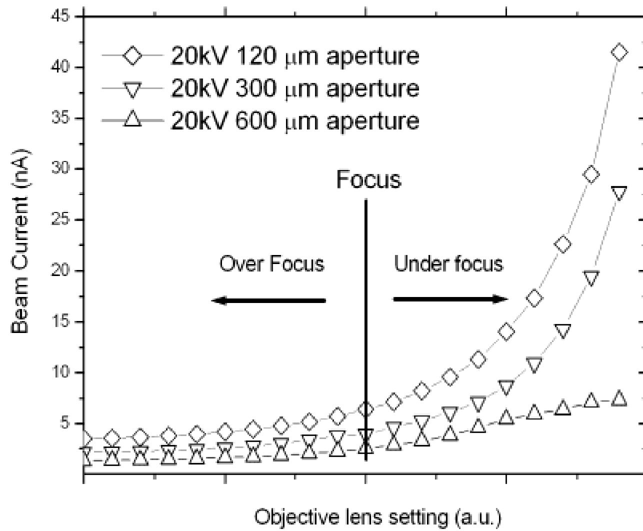


**Figure 7.** Change in $I_B$ as a function of objective lens excitation. $I_B$ increases significantly as the objective lens is taken from under- and overfocus due to the change in the electron beam crossover position with respect to the objective lens aperture.

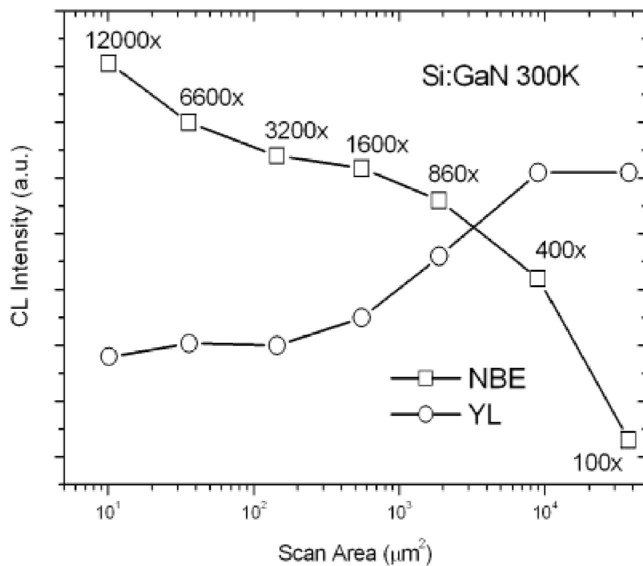


**Figure 8.** The dependence of YL and NBE CL intensity in Si:GaN on SEM magnification. The behavior of the YL band is attributed to its highly nonlinear dependence on the excitation level, whereas the NBE response is tentatively ascribed to competitive recombination with nonradiative surface states, which exhibit a nonlinear dependence on the excitation level ($E_O$ = 20 kV, $I_B$ = 1 nA, CL bandpass = 2.5 nm).

in a SEM, the specimen is not continuously irradiated by the electron beam because of the raster beam-scan mechanism. For a single frame scan, the exposure time ($t_{EX}$) per

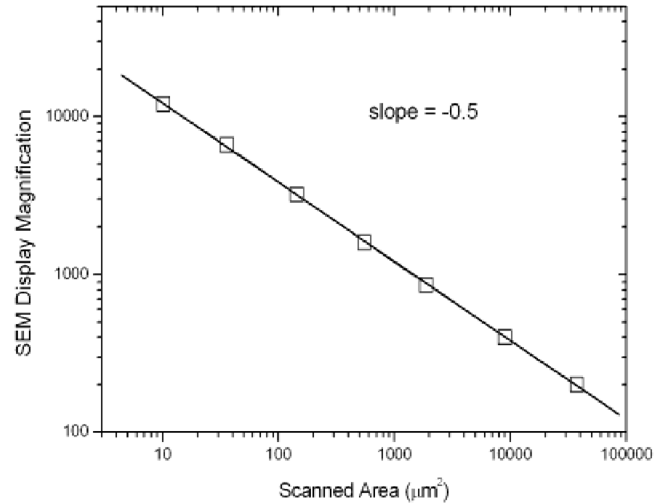


**Figure 9.** The dependence of scan area (in microns) on SEM magnification. The scan area was measured using a calibration mesh.

micron increases with slower line and frame scan speeds, increasing magnification (i.e., decreasing the scan length) and increasing $d_B$ (although in this case there is an associated decrease in the power density of the electron beam). In addition, as each of these factors increase, the time between exposures ($t_{BE}$) following each frame scan decreases, ranging from the frame time to virtually constant irradiation. The magnitude of $t_{EX}$ and $t_{BE}$ can have a significant effect on the saturation rate of recombination centers, depending on the carrier capture rate and recombination lifetimes. However, determination of $t_{EX}$ and $t_{BE}$ is, in general, not a trivial exercise because of the complex electron beam scan methods often used to minimize hysteresis effects in the scan coils. In most SEMs, the beam dwells for a fixed time at the left-hand edge of the frame to allow the scan coils to stabilize before commencing each linescan, producing a highly nonlinear exposure time across the scan. Accurate determination of $t_{EX}$ at each position over the frame scan area therefore requires careful modeling. This work has been completed for the $d_B$, magnification range, and raster scan conditions used in this study, and the results will be presented elsewhere.

## Conclusion

This work shows that the CL intensity of the YL, BL, and DAP bands and the NBE peak in n-type GaN is strongly

dependent on the excitation density, that is, the carrier generation rate per unit volume. Clearly, because of this highly nonlinear relationship between $I_{CL}$ and $I_B$, the intensity ratios between defect-related bands and the NBE in n-type GaN cannot be used to assess the quality of the material or determine the defect concentration. In addition, comparison of different n-type GaN specimens based on CL spectroscopy data can only be reliably undertaken when the spectra are collected under identical SEM operating conditions ($I_B$, $d_B$, $E_O$, magnification, and raster scan). The intensity of the DAP and BL was found to exhibit a square root dependence on excitation density in agreement with theoretical predictions and consistent with experimental PL measurements. However, a cube root dependence on $I_B$ was found for the YL band, which was attributed to the large difference in carrier density and generation rates for electron and optical excitations.

## References


Fleischer, K., Toth, M., Phillips, M.R., Zou, J., Li, G. & Chua, S.J. (1999). Depth profiling of GaN by cathodoluminescence microanalysis. *Appl Phys Lett* **74**, 1114–1116.

Gelhausen, O., Phillips, M.R. & Toth, M. (2001). Depth-resolved cathodoluminescence microanalysis of near-edge emission in III-nitride thin films. *J Appl Phys* **89**, 3535-3537.

Grieshaber, W., Schubert, E.F., Goepfert, I.D., Karlicek, R.F., Jr., Schurman, M.J. & Tran, C. (1996). Competition between band gap and yellow luminescence in GaN and its relevance for optoelectronic devices. *J Appl Phys* **80**, 4615–4620.

Goldstein, J.I., Newbury, D.E., Echlin, P., Joy, D.C., Romig, A.D., Lyman, C.E., Fiori, C. & Lifshin, E. (1992). *Scanning Electron Microscopy and X-ray Microanalysis*, 2nd ed. New York: Plenum.

Herrera Zaldivar, M., Fernandez, P. & Piqueras, J. (1998). Luminescence from growth topographic features in GaN:Si films. *J Appl Phys* **83**, 462–465.

Kim, B., Kuskovsky, I., Herman, I.P., Li, D. & Neumark, G.F. (1999). Reversible ultraviolet-induced photoluminescence degradation and enhancement in GaN films. *J Appl Phys* **86**, 2034–2037.

Neugebauer, J. & Van de Walle, C.G. (1996). Gallium vacancies and the yellow luminescence in GaN. *Appl Phys Lett* **69**, 503–505.

Mullhauser, J.R., Brandt, O., Yang, H. & Ploog, K.H. (1996). Exciton luminescence of single-crystal GaN. In *First International Symposium on Gallium Nitride and Related Materials*, pp. 607–612. Warrendale, PA: Materials Research Society, USA.

Orton, J.W. & Foxon, C.T. (1998). Group III nitride semiconductors for short wavelength light-emitting devices. *Rep Progr Phys* **61**, 1–75.

Pankove, J. (1975). *Optical Processes in Semiconductors*. New York: Dover.

Singh, R., Molnar, R.J., Unlu, M.S. & Moustakas, T.D. (1994). Intensity dependence of photoluminescence in GaN thin films. *Appl Phys Lett* **64**, 336–338.

Reshchikov, M.A. & Korokov, R.Y. (2001). Analysis of the temperature and its excitation intensity dependencies of photoluminescence in undoped GaN films. *Phys Rev B* **64**, 115205–115211.

Toth, M., Fleischer, K. & Phillips, M.R. (1999). Direct experimental evidence for the role of oxygen in the luminescent properties of GaN. *Phys Rev B* **59**, 1575–1578.

Yacobi, B.G. & Holt, D.B. (1990). *Cathodoluminescence Microscopy of Inorganic Solids*. New York: Plenum.

SEARCH RESULTS

ISI Master Journal List
SEARCH RESULTS

Search Terms: 1431-9276
Total journals found: 1

The following title(s) matched your request:

Journals 1-1 (of 1)

FORMAT FOR PRINT

MICROSCOPY AND MICROANALYSIS

Bimonthly
ISSN: 1431-9276
CAMBRIDGE UNIV PRESS, 40 WEST 20TH ST, NEW YORK, USA, NY, 10011-4211

Journals 1-1 (of 1)

FORMAT FOR PRINT